

TECHNIQUE DEVELOPMENT FOR REGULATING THE RATE OF SOLENOIDAL MAGNETIC FIELD DECREASE

N.G. Reshetnyak, V.P. Romas'ko, I.A. Chertishchev

National Science Center "Kharkov Institute of Physics and Technology", Kharkov, Ukraine

E-mail: ch.igor@kipt.kharkov.ua

The problem of regulating the gradient of the solenoidal magnetic field decrease has been investigated in a wide range of values. The results of developing two methods of regulation are reported. With the first method, the field decrease of the main solenoid is regulated through the use of the stray magnetic field, which was produced by SmCO_5 permanent magnets. According to the second method, the regulation was realized with the use of an additional solenoid. The rate of field decrease was regulated within 50...400 Oe/cm. The electron beam formed by the magnetron gun was transported in the decreasing magnetic field of the solenoid. Measuring systems have been created to investigate the beam current distribution in the radial direction.

PACS: 29.17+w

INTRODUCTION

Using the magnetron gun with a secondary-emission cathode as the base, the NSC KIPT team has created the electron accelerator for using the resulting electron beam for irradiation of metallic targets [1, 2]. For practical applications of the electron beams, it is of importance to know the radial distribution of particles in relation to the longitudinal coordinate of the magnetic system. To increase the electron beam current, and consequently, the target specific power, there is a need either to increase the cathode voltage (this is restricted by the interelectrode gap strength of the gun, or to look for other methods of solving the problem). The earlier studies have shown that for increasing the radial beam current density on the tubular surface, it is necessary that the decrease of the magnetic field gradient should be more drastic [3]. With the field created by the solenoid KIU-12, it was possible to attain the field decrease gradient up to 150 Oe/cm. The increase the field decrease gradient up to ≥ 300 Oe/cm calls for the use of an additional solenoid, the longitudinal field of which would be directed in opposite direction to the main solenoidal field or the stray field of the permanent magnets.

COMPUTING, DESIGNING AND MANUFACTURING OF THE ADDITIONAL SOLENOID

Experiments at the electron accelerator were made to investigate the formation of a radial electron beam by the secondary-emission cathode magnetron gun (SECMG) and to measure the parameters of the beam as it is transported in the decreasing magnetic field of the solenoid. The magnetic field for the electron beam generation and transport is created by the solenoid consisting of 4 sections. The sections are power supplied by the dc sources.

Fig. 1 shows the measuring system with the additional solenoid. To provide the required rate of the magnetic field decrease of the main solenoid, the additional solenoid was mounted over the measuring system, inside the vacuum volume. The inner and outer diameters of the additional solenoid were limited by the measuring system size and the inner diameter of the vacuum volume. Note that the facility is assembled so that not only the measuring system by itself, but also the additional

solenoid together with the Faraday cup can be individually moved along the axis (along the magnetic field of the solenoid). Shifting of the additional solenoid and the Faraday cup is possible without deterioration in vacuum. To make the system operate, it took two evacuated connectors to mount on the upper flange of the vacuum volume.

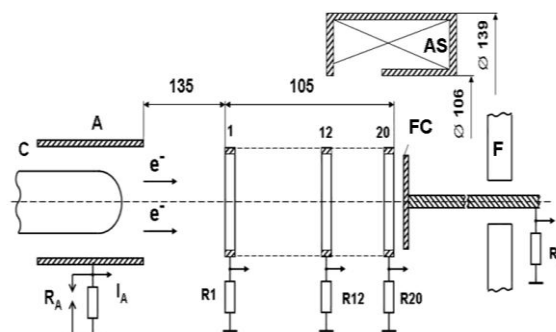


Fig. 1. Arrangement of gun and measuring system components. A – anode; C – cathode; 1-20 – copper rings; FC – Faraday cup; F – flange; R1-R20 – resistive current sensors; R_A – arrester; R_k – Faraday-cup current sensor; AS – additional solenoid

The Faraday cup can move freely along the axis, spanning the distance from the anode edge and onwards behind the last ring. That was provided by the use of a movable vacuum gasket that sealed and insulated the Faraday cup lead (a 10 mm \varnothing polished copper rod) without vacuum failure.

The measuring system consists of copper rings with an inner diameter of 66 mm. The ring width is 8 mm, the separating spacing being 1.5 mm. The rings are insulated relative to each other and from the earth. All the rings are connected to form a single assembly, the length of which makes 130 mm. Provisions are made for both the adjustment of the assembly relative to the cathode axis, and its motion along the axis of symmetry over a distance of ± 100 mm along the axis. The current sensors are composed of low-inductance resistors. The evacuated connectors will receive only the signals from the rings, i.e., the total number of the connector contact groups should be no less than 40, these being connected by thin r.f. cables RC-50-2-12. The anode circuit is protected against occurrence of high voltage in case of the anode-cathode gap breakdown.

Computation and design work was performed for the additional solenoid. The solenoidal field was computed by the program SF7. The computations took into account the geometrical dimensions and coil current of the solenoid, and also, the magnetic screen effect of the solenoid. In this case, the computed and measured field values are in a sufficiently good agreement ($\sim \pm 2\%$).

The magnetic fields of the two (main and additional) solenoids were computed at different geometries of the additional solenoid and its screen. In deciding on the solenoid size, consideration was given to the following limitations: i) the inner diameter of the solenoid is bounded by the measuring system and is equal to 106 mm, ii) the outer diameter is restricted to the inner diameter of the vacuum chamber and is equal to 139 mm.

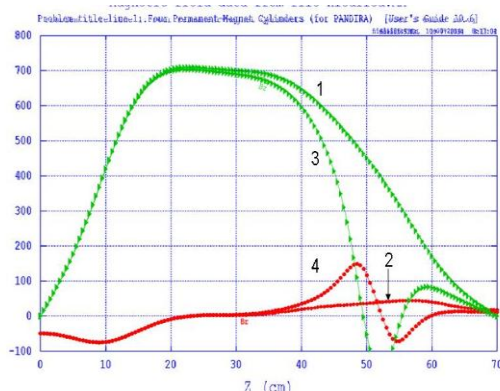


Fig. 2. Computational distributions of longitudinal and radial magnetic fields without using the additional solenoid (curves 1 and 2, respectively), and with the use of the additional solenoid (curves 3 and 4, respectively)

Fig. 2 illustrates the computed distributions of the longitudinal magnetic field with and without the use of the additional solenoid. It is evident from the figure that with the use of the additional solenoid, the rate of the magnetic field decrease increased up to ~ 200 Oe/cm at the rated current in the additional solenoid to be ~ 12 A. Thus, to increase the gradient of the magnetic field decrease, an additional screened solenoid must be used.

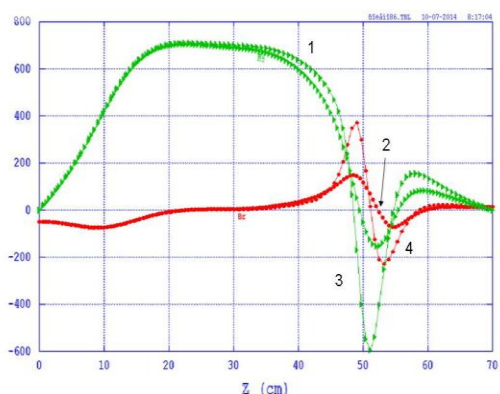


Fig. 3. Longitudinal and radial magnetic field distributions without (curves 1 and 2, respectively) and with the use (curves 3 and 4, respectively) of the magnetic screen of the additional solenoid

Fig. 3 gives the magnetic field distribution with the use of the magnetic screen of the additional solenoid. It can be seen from the figure that the use of the screen can provide a steeper field gradient at a lower current in

the additional solenoid, and that will prevent the additional solenoid from overheating.

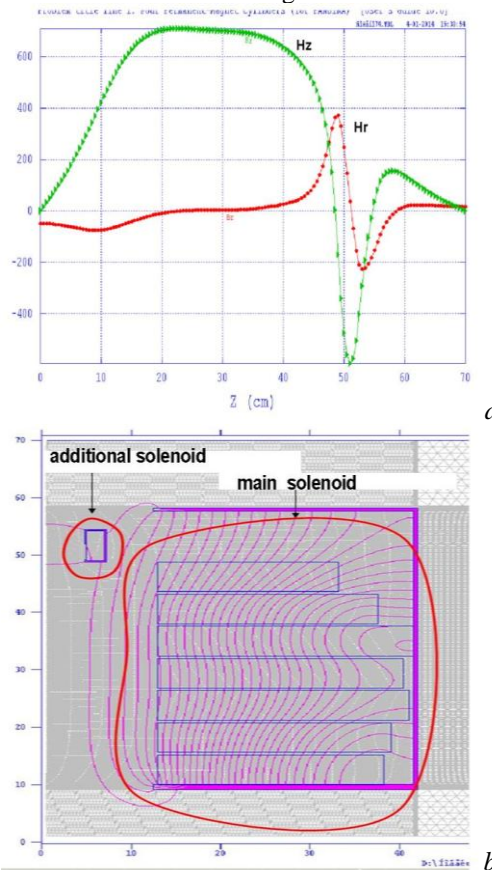


Fig. 4. Computational distributions of longitudinal (Hz) and radial (Hr) magnetic fields in the system having the main solenoid and the additional solenoid (a); geometry of the system comprising the main and additional solenoids (b)

To make the gradient of the magnetic field decrease steeper, the additional solenoid must be encased in a slotted magnetic screen. The calculations have shown that the additional solenoid should be about 70 mm in length, its magnetic screen should be ~ 3 mm thick with ~ 30 mm clearance on its inside part. The calculated magnetic-field distribution was chosen on the basis of the experimental magnetic field. Its value was ~ 700 Oe. Fig. 4,a,b show the chosen solenoid structure and the computational distributions of longitudinal and radial magnetic fields obtained with the given structure.

It is evident from Fig. 3 that the use of the additional solenoid can enhance the magnetic field decrease. When using the additional solenoid with a magnetic screen, the magnetic field decrease is estimated to be ~ 400 Oe/cm. The current of the additional solenoid is estimated in this case to be ~ 12 A.

Fig. 5 shows the external appearance of the additional solenoid with a magnetic screen made from steel ST-3. The solenoid will be able to move along the axis of the system without the break of vacuum. The solenoid winding is coiled using the 1.4 mm \varnothing wire PEV-2. The number of turns of the winding is 265, the ohmic resistance of the winding is $R_0 = 1.15 \Omega$, the winding inductance is $L_0 = 9$ mH.

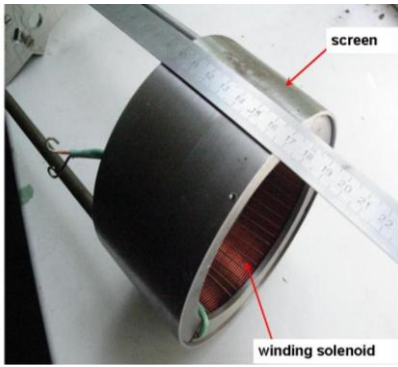


Fig. 5. Screened additional solenoid photograph

Magnetic field measurements of the additional solenoid were performed at three radial distances. Fig. 6 depicts the longitudinal magnetic field distribution at a coil current of 4 A. The maximum field amplitude at a radial distance of 18 mm was measured to be 160 Oe, and at $r = 33$ mm it was 220 Oe.

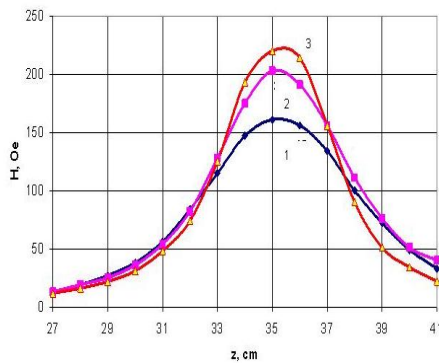


Fig. 6. Longitudinal magnetic field distribution of the additional solenoid at different radial distances: $r_1 = 18$ mm (curve 1), $r_2 = 27$ mm (curve 2), $r_3 = 33$ mm (curve 3)

Fig. 7 shows the normalized magnetic-field peak value at a current of 4 A. It can be seen from the figure that the field amplitude increases linearly (except for the radius 33 m, that can be attributed to field distortions by the solenoid screen).

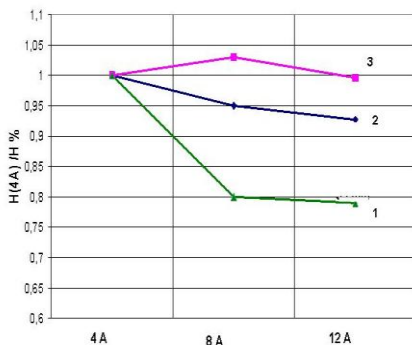


Fig. 7. Normalized magnetic-field peak value at different radial distances: $r_1 = 18$ mm (curve 2), $r_2 = 27$ mm (curve 3), $r_3 = 33$ mm (curve 1)

Magnetic field measurements were also performed for the main solenoid in combination with the additional solenoid. Fig. 8,a shows the longitudinal magnetic field distributions of the main solenoid at its coil currents $I_1 = 48$ A, $I_2 = 0$, $I_3 = 28$ A, $I_4 = -12$ A at a radial distance of 33 mm (curve 1), and also the distributions of the combined field of the main and additional solenoids (curves

2 to 4). The current values of the additional solenoid were preset to be $I_1 = 0$ (curve 2), $I_2 = 4$ A (curve 3), $I_3 = 8$ A (curve 4). It is evident from the figure that the introduction of the screen distorts the solenoidal field. Thus, in the presence of the screen, the longitudinal field amplitude decreases from 250 Oe down to 80 Oe over the distance of 35 cm from the anode edge. At $I_3 = 8$ A of the additional solenoid, the maximum gradient of the magnetic field decrease was found to be ~ 300 Oe/cm. Fig. 8,b gives the combined magnetic field distributions of the solenoids KIU-12 and the additional solenoid at the main solenoid coil currents $I_1 = 30$ A, $I_2 = 0$, $I_3 = 22$ A, $I_4 = 34$ A, and at additional solenoid currents $I_1 = 0$ (curve 1), $I_2 = 4$ A (curve 2), $I_3 = 8$ A (curve 3). It is seen from the figure that in this case the maximum rate of field decrease (300 Oe/cm) has also been gained.

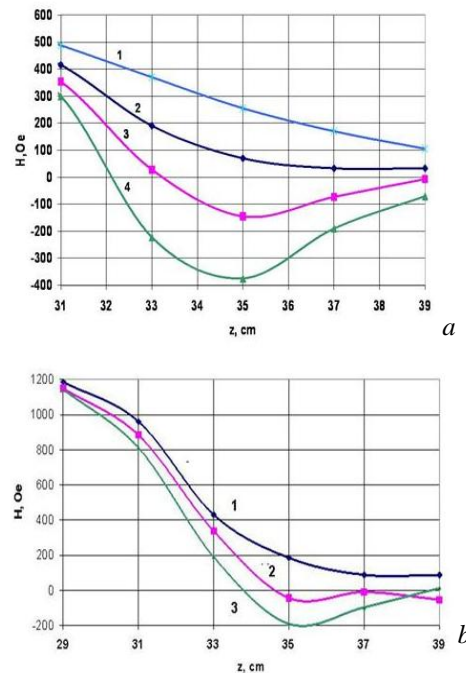


Fig. 8. Combined longitudinal magnetic field distribution of the main solenoid and the additional solenoid in the region of the maximum gradient of the field decrease

Considering that the additional solenoid will be operated without forced cooling, it was necessary to perform measurements of the solenoid operating temperature. Fig. 9,a shows the heating versus time relationship at the solenoid current 8 A. Within 8 minutes the solenoid heated up from 25 up to 67°C, and then for the time of 25 minutes it cooled down to 45°C. Besides, it was of concern to measure the temperature dependence at the operation conditions close to the working regime. The beam operation time, equal to 2 minutes, is followed by the 5-min operation of the setup under no-load conditions, without any beam generation. During this period, the vacuum chamber is being evacuated and the solenoid cools down. Fig. 9,b shows the solenoid heating as a function of time at the given working mode cycle. It is obvious that for 3 cycles of operation at these conditions the solenoid will heat up from 42 up to 59°C.

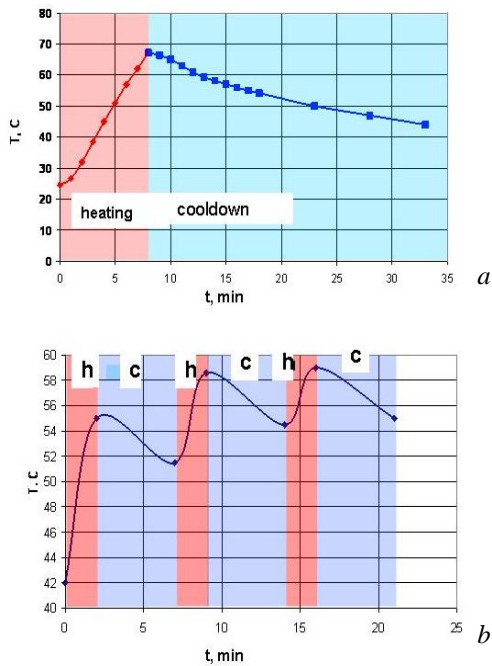


Fig. 9. Time dependence of the solenoid heating and cooldown at continuous operation of the solenoid (8 minutes) and at cycling (2 minute heating – 5 minute cooldown)

Fig. 10 show longitudinal magnetic field distributions and geometry of the system and current histograms at these distributions. Use of the additional solenoid makes it possible to increase the flow of electrons per ring.

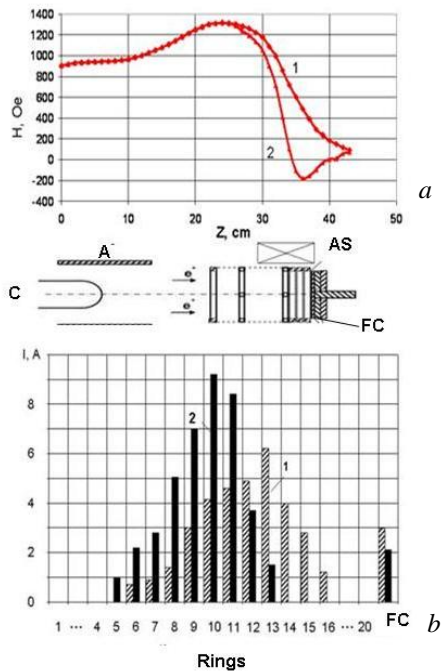


Fig. 10. Longitudinal magnetic field distributions and geometry of the system: A – anode; C – cathode; FC – Faraday cup; AS – additional solenoid (a). Current histograms at these distributions (b)

FIELD REGULATION BY PERMANENT MAGNETS

Another method of regulating the rate of magnetic field decrease consisted in using the scattered magnetic

field of annular SmCO_5 magnets, which were placed on the axis of the system. Fig. 11,a shows the longitudinal distributions of the stray magnetic field of two annular magnets at different radial distances ($r = 20, 25, 30, 33$ mm). It can be seen from the figure that the maximum field amplitude at $r = 20$ mm is equal to 700 Oe, while at $r = 33$ mm it equals 150 Oe. The stray magnetic field measurements were performed with the annular magnets of different geometrical dimensions. The measurements have pointed to the possibility of using the stray magnetic field of two annular magnets for regulating the gradient of the magnetic field decrease during the formation of the electron beam in the radial direction as the beam is transported in the decreasing field of the solenoid.

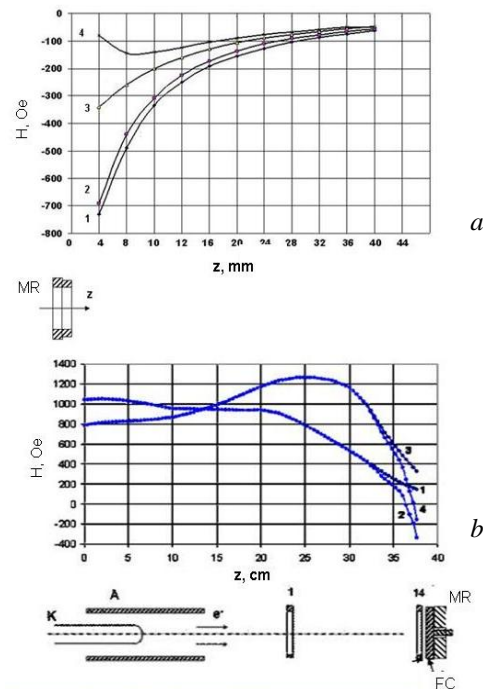


Fig. 11. Distributions of the combined longitudinal stray magnetic field of two annular magnets at different radii (1 – $r = 20$ mm; 2 – $r = 25$ mm; 3 – $r = 30$ mm; 4 – $r = 33$ mm) at the distance $z = 4$ mm from the magnet assembly surface

The distribution of the magnetic field created by the solenoid and annular magnets (see Fig. 11, curve 4), and the gradient of its decrease can be optimized by increasing the number of electrons incident on one ring (up to 70% of the beam current).

The experimental studies on electron beam formation with increasing gradient of the magnetic field decrease have been carried out.

CONCLUSIONS

An additional solenoid has been designed and manufactured. In combination with the main solenoid, it enables one to increase the rate of the magnetic field decrease up to 400 Oe/cm.

Electron beam experiments have been made to prove that the use of the additional solenoid or permanent magnets makes it possible to increase the flow of electrons per ring.

REFERENCES

1. A.N. Dovbnya, V.V. Zakutin, N.G. Reshetnyak, V.P. Romas'ko, I.A. Chertishchev, V.N. Boriskin, N.A. Dovbnya, T.A. Kovalenko. Studies on beam formation in the electron accelerator with the secondary-emission source // *Announcer of the Kharkov National University. Series Physics "Kernels, particle field"*. 2006, № 732, iss. 2(30), p. 96-100.
2. A.N. Dovbnya, S.D. Lavrinenko, V.V. Zakutin, et al. Zirconium and Zr1%Nb alloy surface modification by the electron beam of the magnetron gun-based accelerator // *Problems of Atomic Science and Technology. Series "Physics of Radiation Damages and Radiation Materials Science"*. 2011, № 2, p. 39-45.
3. N.I. Aizatsky, V.N. Boriskin, A.N. Dovbnya, et al. Formation of radial electron beam by the secondary-emission magnetron gun: experiment and theory // *Appl. Radioelectronics*. 2014, v. 13, № 2, p. 127-34.

Article received 09.03.2016

РАЗРАБОТКА СПОСОБОВ РЕГУЛИРОВКИ СКОРОСТИ СПАДА МАГНИТНОГО ПОЛЯ СОЛЕНОИДА

Н.Г. Решетняк, В.П. Ромасько, И.А. Чертищев

Рассматривалась задача регулировки градиента спада магнитного поля соленоида в широком интервале значений. Приведены результаты разработки двух методов регулировки. В первом из них для регулировки спада поля основного соленоида использовано рассеянное магнитное поле, которое создавалось постоянными магнитами из SmCO_5 . Во втором методе регулировка осуществлялась с помощью дополнительного соленоида. Скорость спада регулировалась в пределах 50...400 Э/см. Транспортировка электронного пучка, формируемого магнетронной пушкой, осуществлялась в спадающем магнитном поле соленоида. Созданы измерительные системы для исследования распределения тока пучка в радиальном направлении.

РОЗРОБКА СПОСОБІВ РЕГУЛЮВАННЯ ШВИДКОСТІ СПАДУ МАГНІТНОГО ПОЛЯ СОЛЕНОЇДА

М.Г. Решетняк, В.П. Ромасько, І.О. Чертіщев

Розглядалася задача регулювання градієнта спаду магнітного поля соленоїда в широкому інтервалі значень. Наведено результати розробки двох методів регулювання. У першому з них для регулювання спаду поля основного соленоїда використано розсіяне магнітне поле, яке створювалося постійними магнітами з SmCO_5 . У другому методі регулювання здійснювалося за допомогою додаткового соленоїда. Швидкість спаду регулювалася в межах 50...400 Е/см. Транспортування електронного пучка, який формується магнетронною гарматою, здійснювалося в спадаючому магнітному полі соленоїда. Створені вимірювальні системи для дослідження розподілу струму пучка в радіальному напрямку.